Depth and Arbitrary Motion Deblurring Using Integrated PSF

Takeyuki Kobayashi, Fumihiko Sakaue, Jun Sato

Department of Computer Science and Engineering, Nagoya Institute of Technology

Abstract. In recent years, research for recovering depth blur and motion blur in images has been making a significant progress. In particular, the progress in computational photography enabled us to generate all-in-focus images and control depth of field in images. However, the simultaneous recovery of depth and motion blurs is still a big problem, and recoverable motion blurs are limited.
In this paper, we show that by moving a camera during the exposure, the PSF of the whole image becomes invariant, and motion deblurring and all-in-focus imaging can be achieved simultaneously. In particular, motion blurs caused by arbitrary multiple motions can be recovered. The validity and the advantages of the proposed method are shown by real image experiments and synthetic image experiments.

Keywords: Coded imaging, PSF, Deblur, Motion Blur , All-in-Focus

1 Introduction

Deblurring depth and motion blurs is very important in many applications. In order to deblur depth blur and motion blur, various methods have been studied in recent years. Many methods use specific models of PSF (Point Spread Function) for representing the blur. By using the PSF, blurred images can be represented by convolution of the PSF and the sharp (all-in-focus) images. Thus, deblurring of the image can be achieved by deconvolution of the PSF. However, the PSF is in general not unique for a whole image, since the PSF depends on the depth of objects. In order to suppress the variation of PSFs, some methods based on the light field computation were proposed[4, 1] in recent years. Although these methods can deblur observed images with various depth, we need to obtain multiple images which are captured under different blurring conditions.

The image deblurring has also been studied in computational photography in recent years[8, 9]. Veeraraghavan et al.[9] proposed the coded aperture for image deblurring. They focused on the zero-cross in the frequency characteristics of PSF in coded aperture, and optimized the coded aperture by decreasing the zero-cross. Nagahara et al.[6] proposed focus sweep imaging for expanding the depth of field. In their method, the image sensor (image plane) in a camera moves during exposure. By this movement, the PSF on an image plane becomes approximately invariant under change in depth. Thus, we can deblur observed images easily by using a single PSF all over the image. However, we need to

move the image sensor in a camera device quickly, and thus it is not easy to implement by using ordinary camera systems.

The motion blur occurred by relative motions between cameras and objects has also been studied. Raskar et al.[7] proposed coded exposure for deblurring the motion blur accurately. They proposed a method for controlling a shutter during exposure, i.e. coded exposure. By using the coded exposure, the quality of deblurred images can be improved. However, the obtained images become darker, since the exposure time becomes a half of the original exposure time, and the S/N ratio of obtained image becomes worse. Furthermore, we have to obtain the image motion beforehand in order to optimize the coded exposure. Levin et al.[5] showed that the PSF of motion blur becomes invariant under image motions, if the camera moves along with a parabolic orbit. Although the method works well when we know the orientation of the object motions, arbitrary unknown motions cannot be deblurred. Cho et al.[3] proposed an imaging technique which enables us to obtain invariant motion blurs under arbitrary 2D image motions and deblur them. However, we need to obtain two different images moving the camera with parabolic motions in two orthogonal directions. Bando et al.[2] proposed a method for estimating motion blur by using circular motion of image sensor. Although we can estimate PSF of motion blur by using this method, the method cannot be applied when we have complex motions in the scene.

In this paper, we propose a method for deblurring depth and motion blurs simultaneously. In particular we propose a method for deblurring motion blurs caused by complex multiple motions of objects. In this research, we use the focus sweep technique proposed by Nagahara et al.[6], and show that we can recover not only depth blurs but also motion blurs simultaneously by using the focus sweep technique. We also show that it enables us to deblur not only a single motion in images, but also arbitrary multiple motions in images simultaneously. Furthermore, we clarify the condition of deblurring the mixture of depth and motion blurs in images, which is very useful for designing the imaging systems. The method is tested by using real images and synthetic images generated by a lens simulator.

2 Lens model

In this paper, we first consider a bilateral telecentric lens in order to simplify the explanation of our method, and then generalize it to ordinary perspective lens systems.

We first explain the characteristics of a bilateral telecentric lens, which is shown in Fig. 1. The focal lengths of lens 1 and lens 2 are f_1 and f_2, and these lenses are placed at their respective focal distances from the aperture to form a bilateral telecentric lens system. Let a be the diameter of aperture, p be the distance between the image sensor and Lens 2, u be the distance between the object and Lens 1. Then, all the incident lights are concentrated at point A, whose distance is v_1 from Lens 1, and u_2 from Lens 2, and are finally concentrated at a point whose distance is v_2 from Lens 2 as shown in Fig. 1. Then, the following

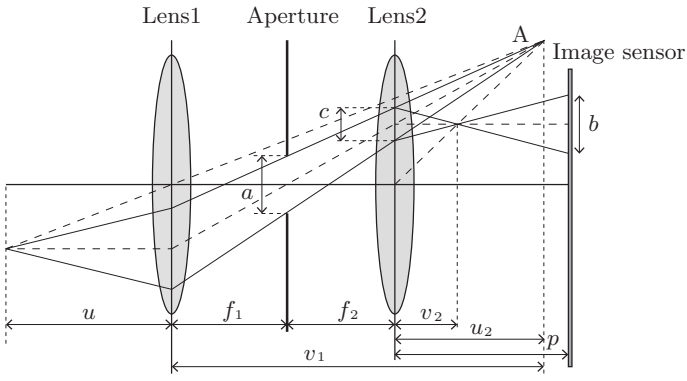

Fig. 1. Bilateral telecentric lens.

equations hold for these lenses.

$$\frac{1}{f_1} = \frac{1}{u} + \frac{1}{v_1} \tag{1}$$

$$\frac{1}{f_2} = -\frac{1}{u_2} + \frac{1}{v_2} \tag{2}$$

By using these equations and geometric relationships shown in Fig. 1, we have the following equation, which shows the diameter of a blurred circle b introduced by the lens system.

$$b = a\left|\frac{f_2 u}{f_1^2} + \frac{p}{f_2} - \frac{f_2}{f_1} - 1\right| \tag{3}$$

3 IPSF

By using the telecentric lens model shown in the previous section, we next consider the PSF of an image under focus sweep imaging. In this method, image plane moves along with light axis during exposure, and thus, observed PSF can be described by the integration of PSF which changes according to the image plane motion. In this paper, we call the integrated PSF as IPSF following [6].

Let us consider the case where a 3D point $\mathbf{X}$ is projected to $\mathbf{m}$ in the image. If we have image blur, the point in the image is spread, and the observed intensity at $\mathbf{x} = [x, y]^\top$ can be described by the pill box function as follows:

$$P(r, u, p) = \frac{4}{\pi b^2} \Pi\left(\frac{r}{b}\right) \tag{4}$$

where r is the distance between $\mathbf{x}$ and $\mathbf{m}$, and b denotes the radius of the image blur. Note, the radius b is determined by u and p, which are the distance between

the lens and the object, and the distance between the lens and the image sensor, as shown in Eq.(3). The function $\Pi(w)$ is a pill box function, which is described as follows:

$$\Pi(w) = \begin{cases} 1, & |w| < \frac{1}{2} \\ 0, \text{ otherwise} \end{cases} \tag{5}$$

The Eq.(4) indicates that observed PSF depends on the distance u, and thus, the PSF is not unique for whole image because the depth u changes pixel by pixel in general scene.

Now, let us consider the case where the distance u or p changes linearly during image exposure. Let us denotes the distance u at time t as $u(t)$, and p at time t as $p(t)$. Then, the integrated PSF (IPSF) can be described as follows:

$$IP(r) = \int_{T_1}^{T_2} P(r, u(t), p(t))dt \tag{6}$$

where T_1 denotes shutter opened time and T_2 denotes shutter closed time, and thus the exposure time is $T = T_2 - T_1$.

For example, if the camera translates along with light axis with a uniform speed s_u, then the changes of distance u can be described as follows:

$$u(t) = u_0 + s_u t \tag{7}$$

where u_0 indicate a distance from the camera to the object at $t = 0$. In this case, the change in size of blur is constant, and thus Eq.(3) can be rewritten as follows:

$$b(t) = |2s_b t| \tag{8}$$

where, s_b denotes the speed of the change in radius of blur.

4 Invariance of IPSF under 3D Motions

We next show that IPSF under focus sweep imaging is invariant against speed, direction and depth if some conditions are satisfied. In this section, we analyze the characteristics of IPSF and derive the conditions in which the IPSF becomes invariant.

Let us consider the case where a moving 3D point is projected onto the image plane. The 3D point at t is denoted by $\mathbf{X}(t)$ and the projected point is denoted by $\mathbf{m}(t) = [u, v]^\top$. In this case the PSF of a projected point at t can be described as follows:

$$P(\mathbf{x}, u, p) = \frac{4}{\pi b(t)^2} \Pi \left(\frac{||\mathbf{x} - \mathbf{m}(t)||}{b(t)} \right) \tag{9}$$

In this equation, we described the PSF by using the observed point $\mathbf{x}$ and the center of blur $\mathbf{m}(t)$, since the center of blur $\mathbf{m}(t)$ also moves in time. From the

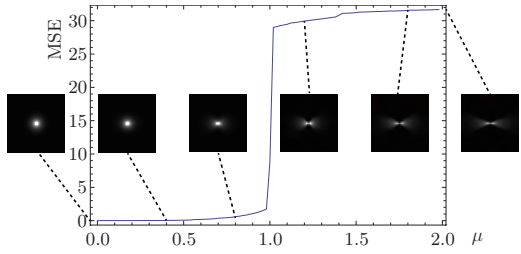

Fig. 2. The relationship between IPSF and the speed ratio μ.

integration of this function with respect to t, the IPSF can be computed as follows:

$$IP(\mathbf{x}) = \int_{T_1}^{T_2} \frac{4}{\pi b(t)^2} \Pi\left(\frac{||\mathbf{x} - \mathbf{m}(t)||}{b(t)}\right) dt \tag{10}$$

Suppose the motion of the projected point $\mathbf{m}(t)$ can be described linearly by using its speed s_m and direction $\mathbf{v}$ on the image sensor. Then, the motion of the point $\mathbf{m}(t)$ can be described as follows:

$$\mathbf{m}(t) = s_m t\, \mathbf{v} \tag{11}$$

Now, if the camera moves linearly with a speed s_u along with the light axis, the size of blur changes linearly as shown in Eq.(8). Thus, the IPSF can be computed from Eq.(8), Eq.(11) and Eq.(10) as follows:

$$IP(\mathbf{x}) = \frac{1}{\pi s_b^2}\left\{\lambda_0\left(\frac{1}{|t_0|} - \frac{2}{T}\right) + \lambda_1\left(\frac{1}{|t_1|} - \frac{2}{T}\right)\right\} \tag{12}$$

where t_0 and $t_1(|t_1| > |t_0|)$ are the solutions of a quadratic equation $|\mathbf{x} - s_m t\, \mathbf{v}|^2 = s_b^2 t^2$, and λ_0 and λ_1 are variables which are described as follows:

$$t_{0,1} = \frac{-s_m \mathbf{x}\cdot\mathbf{v} \pm \sqrt{s_m^2(\mathbf{x}\cdot\mathbf{v})^2 + |\mathbf{x}|^2(s_b^2 - s_m^2)}}{s_b^2 - s_m^2} \tag{13}$$

$$\lambda_0 = \begin{cases} 1, & |t_0| < \frac{T}{2} \\ 0, \text{ otherwise} \end{cases} \tag{14}$$

$$\lambda_1 = \begin{cases} 1, & (|t_1| < \frac{T}{2}) \wedge (t_0 t_1 < 0) \\ -1, & (|t_1| < \frac{T}{2}) \wedge (t_0 t_1 > 0) \\ 0, & \text{otherwise} \end{cases} \tag{15}$$

If the exposure time of camera is sufficiently small, arbitrary motions can be approximated by linear motions. Thus, Eq.(12) covers all the motions.

By using the IPSF model described in Eq.(12), we next consider the relationship between the IPSF and a speed ratio μ. The speed ratio μ is defined as

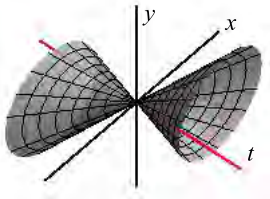

Fig. 3. Changes in PSF ($\mu = 0.8$)

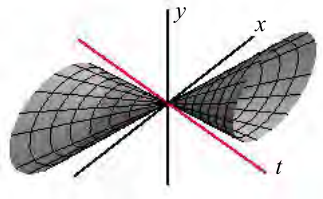

Fig. 4. Changes in PSF ($\mu = 1.4$)

follows:

$$\mu = \left| \frac{s_m}{s_b} \right| \tag{16}$$

and it represents the relative speed between the speed of projected point s_m and the speed of the change in radius of blur s_b.

Fig. 2 shows the relationship between the speed ratio μ and the change in IPSF, that is the difference between the IPSF of a static object and the IPSF of a moving object. Fig. 2 shows that the IPSF is almost unchanged when μ is smaller than 1, although it changes drastically when μ is larger than 1. Furthermore, the IPSF is almost isotropic when μ is smaller than 1, while it is unisotropic when μ is larger than 1. Thus, we find that the IPSF can be considered as invariant when the following condition holds:

$$\mu \leq 1 \tag{17}$$

Thus, if this condition holds, we can deblur image blurs caused by arbitrary motions just by deblurring with a uniform IPSF all over the image.

Let us consider the reason why invariance breaks when the speed ratio μ becomes larger than 1. The weight of PSF at each time in IPSF is not equivalent in general. For example, the value of $P(\mathbf{x}, u, p)$ becomes extremely large when the target object is at the focus position. On the other hand, the value of $P(\mathbf{x}, u, p)$ becomes very small when the target object is far from the focus position. Thus, the IPSF heavily depends on the PSF at focus position. When object speed s_m is smaller than the speed of blur s_b, the changes in PSF (which is pill box function) can be described as shown in Fig. 3. In this case, the time axis t (which is the center of blur) is in a cone which represents the PSF, and thus, the center of blur is always in the PSF during the motion. Thus, IPSF is approximately invariant, even if the motions are different. However, if s_m becomes larger than s_b, the time axis t is out of the PSF cone as shown in Fig. 3. Thus, the IPSF changes drastically depending on the motions. As a result, Eq.(17) is the critical condition for the invariance of IPSF.

5 Invariant IPSF By Using Ordinary Lens

We next generalize our analysis into ordinary perspective lens from bilateral telecentric lens. When we use ordinary lenses for image projection, the position

of projected points depends on not only horizontal and vertical positions of object, but also the depth u of object. Therefore, if the image plane or the whole camera moves along with the light axis, projected points also moves even if the 3D point is static.

However, the motion of a projected point by using the ordinary lens can be regarded as a radial motion of target object under telecentric lens. Thus, the IPSF becomes invariant, if the radial motion satisfies the condition described in the previous section.

Let us describe the image motion of the projected point caused by the change in depth u by using the direction $\mathbf{u}$ and the speed s_z. Then, the motion of the projected point can be described by the summation of the motion $s_z\mathbf{u}$ caused by the change in depth and the motion $s_m\mathbf{v}$ caused by the object motion as follows:

$$s_a\mathbf{w} = s_m\mathbf{v} + s_z\mathbf{u} \tag{18}$$

where, $\mathbf{w}$ denotes the direction of the combined motion, and s_a denotes the speed of the combined motion.

Now, we define the speed ratio μ as follows:

$$\mu = \left| \frac{s_a}{s_b} \right| \tag{19}$$

Then, the focus point is always in the blur circle, when the following condition holds:

$$\mu \leq 1 \tag{20}$$

Thus, we find that the IPSF is invariant under ordinary perspective lens systems, when Eq.(20) is satisfied, and we can deblur images by using a uniform IPSF, even if we have arbitrary multiple motions in the scene.

6 Experimental Result Using Synthesized Images

In this section, we evaluate the proposed method by using synthetic images. We made a lens simulator which can simulate arbitrary lens systems, and generated synthetic images of objects under the focus sweep. The object is a planar surface, and some characters are printed on this plane. For comparison, images taken by the method proposed by Levin et al.[5] were also synthesized. The synthesized images are shown in Fig. 5 and Fig. 6. These images were synthesized under various motions of object surface, i.e. (a) static, (b) horizontal motion, (c) vertical motion, (d) diagonal motion, (e) rotational motion and (f) zoom. In the proposed method, the camera moved 11mm during exposure. The telecentric lens was used and its focus lengths are $f_1 = 60$ mm and $f_2 = 60$ mm respectively. The size of aperture was $a = 10$ mm. In Levin's method, the camera moved in horizontal parabolic orbit. The Gaussian noises with the std of $\sigma = 0.1$ were added to each image intensity. The maximum value of the speed ratio μ was (a) 0, (b) 0.45, (c) 0.46, (d) 0.65, (e) 0.98 and (f) 0.86, thus all of them satisfied the proposed condition. Wienner filter was used for deconvolution in both methods.

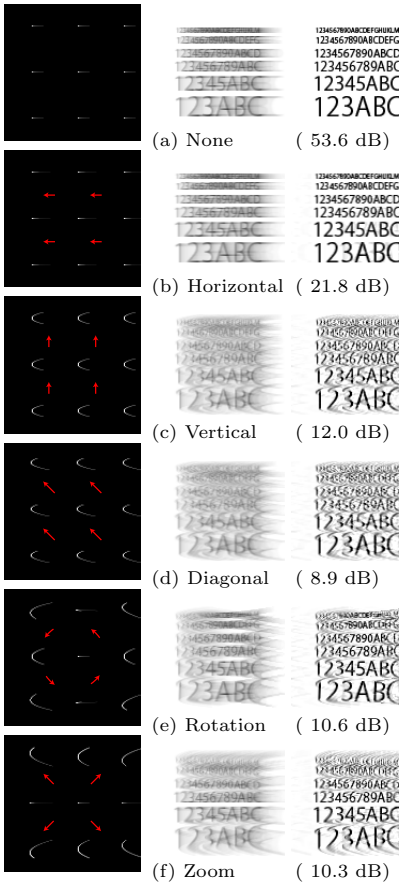

Fig. 5. Images deblurred by Levin's method: IPSF (left), observed images (center) and deblurred results (right).

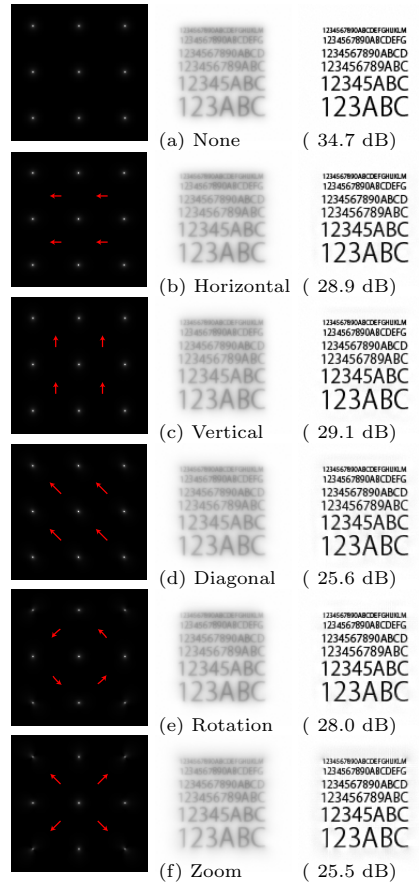

Fig. 6. Image deblurred by the proposed method: IPSF (left), observed images (center) and deblurred result.

The PSNR of deblurred images were computed and they are represented under the each result.

As shown in Fig. 5, although Levin's method provides us good results in horizontal motion, it does not work well in other motions. This is because the horizontal parabola was used in Levin's method, and it cannot deblur images under other motions. In contrast, the proposed method provides us very good results under all the motions as shown in Fig. 6. In particular, change of scale and rotation, which cannot be deblurred properly by the ordinary deblurring methods can be deblurred properly by our method. From these results, we find that the proposed method can deblur arbitrary unknown motions when the condition described in Eq.(20) holds.

(a) μ=0 (b) μ=0.5 (c) μ=0.9 (d) μ=1.1 (e) μ=1.5 (f) μ=2.0

Fig. 7. Image deblurring results under various speed ratio μ. When μ is smaller than 1.0, images can be deblurred properly.

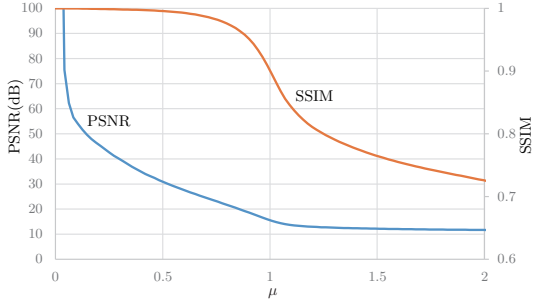

Fig. 8. Relationship between speed ratio and PSNR/SSIM of deblurred images.

We next evaluate the robustness of the proposed method against changes in object speed. In this experiment, the speed ratio μ was changed from 0 to 2.0, and observed images were deblurred by the proposed method. Fig. 7 shows the deblurred images under each speed ratio μ. As shown in Fig. 7, the image blur was recovered properly in (a), (b) and (c), while it was not recovered properly in (d), (e) and (f). This is because the speed ratios of (d), (e) and (f) are over 1.0, and they do not satisfy the condition for image deblurring. These results show that the deblurring condition derived in this paper is valid.

Fig. 8 shows the relationship between the speed ratio μ and the accuracy of deblurring. In this figure, the vertical axis shows the PSNR and SSIM[10] of deblurred images. This figure shows that the quality of image deblurring depends on the speed ratio. In particular, SSIM of deblurred images changes drastically at around $\mu = 1.0$, and thus, we find that the limitation of μ exists at around 1.0.

7 Experimental results by Using Real Devices

We next show experimental results from real camera systems. We first show results when we used telecentric lens for the camera system. The camera system and a target object were fixed on a translation/rotation stage as shown in Fig. 9.

Fig. 9. The camera system for obtaining images.

(a) No motion (b) With motion (c) Levin's method (d) IPSF image (e) Deblurred image

Fig. 10. Experimental results by using a real camera system: Target objects were moved horizontally (top row), vertically (middle row) and rotationally (bottom row).

The target object was moved horizontally, vertically and rotationally. The camera system was moved in the proposed method, and the speed of the motion was $s_u = 300$ mm/sec. The exposure time of the camera was 0.5 sec. For comparison, the camera was moved according to Levin's method and took images. The zoom of the telecentric lens was 0.17, W.D = 113 mm, depth of field is 11 mm and F=4.0. The size of CCD of the camera was 1/2".

Fig. 10 shows the observed images and the deblurred images. (a) shows the observed images from fixed cameras and fixed objects, (b) shows the images of a moving objects taken from a fixed camera, (c) shows the deblurred result by Levin's method, (d) shows the IPSF images taken by a moving camera and (e) shows the deblurred result by the proposed method. Note, the depth of the target object is larger than 11 mm, which is the depth of field of the camera, and thus, some pixels have depth blur even if the target object is static. In the results of Levin's method shown in (c), although the horizontal motion blur could be recovered, the depth blur remains in the image. In addition, vertical

(a) Experimental system (b) IPSF image (c) Deblurred image (d) Normal imaging

Fig. 11. Experimental results by using the ordinary perspective lens. (a) shows translation stage used for obtaining images, (b) is the observed IPSF image, (c) is the deblurred image derived from the proposed method and (d) is the image taken by the ordinary camera system.

and rotational motion blur could not be recovered. In contrast, the proposed method could deblur properly in any motion blurs as long as the blur satisfies the condition. Furthermore, the depth blur could also be recovered by the proposed method.

We next show deblurring results when we used an ordinary perspective lens for a camera system. In this case, our method can deblur image when Eq.(20) is satisfied. In this experiment, the camera system was moved by using a translation stage as shown in Fig.11 (a), and the IPSF images were obtained by using the moving camera system. The example of the observed image is shown in Fig. 11 (b) and the deblurred result is shown in (c). For comparison, the normal exposure image is shown in Fig. 11. As shown in this image, the proposed method can deblur images, even if they include many different motion blurs. The result indicates that our proposed method can deblur arbitrary motion blurs as long as the blur satisfies the condition Eq.(20).

8 Conclusion

In this paper, we proposed a method for obtaining invariant IPSF image by using camera motion during exposure. By using the method, the IPSF of the image becomes uniform, and thus, we can deblur whole image by using a single IPSF. Furthermore, we analyze properties of the IPSF and derived the condition for obtaining invariant IPSF image. The method can apply not only a camera with a telecentric lens, but also an ordinary perspective lens. The experimental results show that the proposed method can deblur not only arbitrary motion blur but also depth blur.

References

1. A.Levin, F.Durand: Linear view synthesis using a dimensionality gap light field prior. IEEE CVPR pp. 1831–1838 (2010)
2. Bando, Y., Chen, B.Y., Nishita, T.: Motion deblurring from a single image using circular sensor motion. Computer Graphics Forum (Proceedings of Pacific Graphics) 30(7), 1869–1878 (2011)
3. Cho, T., Levin, A., Durand, F., Freeman, W.T.: Motion blur removal with orthogonal parabolic exposures. IEEE International Conf. on Computational Photography (ICCP) pp. 1–8 (2010)
4. K.Kodama, H.Mo, A.Kubota: Simple and fast all-in-focus image reconstruction based on three-dimensional/two-dimensional transform and filtering. IEEE ICASSP 1, 769–772 (2007)
5. Levin, A., Sand, P., Cho, T., Durand, F., Freeman, W.: Motion-invariant photography. SIGGRAPH, ACM Trans. Graphics (2008)
6. Nagahara, H., Kuthirummal, S., Zhou, C., Nayar, S.K.: Flexible depth of field photography. Proc. Europian Conf. Computer Vision LNCS(5305), 60–73 (2008)
7. Raskar, R., Agrawal, A., Tumblin, J.: Coded exposure photography: Motion deblurring using fluttered shutter. ACM Trans. Graphics 25, 795–804 (2006)
8. Subbarao, M., Surya, G.: Depth from defocus: A spatial domain approach. International Journal of Computer Vision 13(3), 271–294 (1994)
9. Veeraraphavan, A., Raskar, R., Agrawal, A., Mohan, A., Tumblin, J.: Dappled photography : Mask enhanced cameras for heterodyned light fields and coded aperture refocusing. ACM Trans. Graphics (2007)
10. Wang, Z., Bovik, A.C., Sheikh, H.R., Simoncelli, E.P.: Image quality assessment: From error visibility to structural similarity. IEEE Transactions on Image Processing 13(4), 600–612 (2004)